

## Mechanical Behavior of Long Carbon Fiber Reinforced Polyarylamide at Elevated Temperature

Wang Q<sup>1</sup>, Ning H<sup>1\*</sup>, Vaidya U<sup>2</sup> and Pillay S<sup>1</sup>

<sup>1</sup>Department of Materials Science and Engineering, University of Alabama at Birmingham, Birmingham, USA

<sup>2</sup>Department of Mechanical, Aerospace and Biomedical Engineering, University of Tennessee, Knoxville, USA

### Abstract

Long fiber reinforced thermoplastic (LFT) composites have recently found increasing use in transportation, military and aerospace applications and become well established as high volume and low cost materials with high specific modulus and strength, superior damage tolerance, and excellent fracture toughness. This study is conducted to evaluate the performance of long fiber reinforced thermoplastic composite at elevated high temperature. Long carbon fiber reinforced polyarylamide (CF/PAA) composites containing 20 wt% and 30 wt% carbon fibers are used and processed using extrusion compression molding. Flexural and tensile samples are tested at three temperatures, room temperature, medium temperature (MD 65°C) and glass transition temperature (TG 80°C). Samples in both longitudinal and transverse directions are prepared to show the effect of the orientation on mechanical properties at different temperatures. The testing results show that as temperature increases, both of the flexural and tensile properties of the CF/PAA decrease as expected. Both of the flexural and tensile modulus reduce more dramatically than the flexural and tensile strength, indicating that the temperature has more pronounced effect on modulus than strength. The transversely oriented samples generally show larger reduction in properties than the longitudinally oriented samples. Temperature significantly affects flexural strength at the elevated temperature section between MD and TG temperature.

**Keywords:** Long carbon fibers; Thermoplastic; Polyarylamide; PA-MXD6; Mechanical properties; Elevated temperature

### Introduction

Long fiber reinforced thermoplastic (LFT) is a class of composite material comprised of reinforcement fibers (carbon and glass fibers etc.) and thermoplastic polymers such as polypropylene (PP), polyamide (PA), and polyphenylene sulfide (PPS), etc. The reinforcement fibers are typically 5-25 mm in length with resultant high fiber aspect ratio, compared to 0.5-1.0 mm in short fiber reinforced thermoplastic (SFT). The long fibers in LFT composites provide several property advantages, such as high impact strength, improved modulus and better dimensional stability, over SFT composites. LFT is manufactured by pulling continuous fiber tows through a thermoplastic polymer melt in a processing die. The ratio of fiber to resin is controlled by a metering orifice. The resulting rods are cut into pellets, 5-25 mm in length, which can be injection molded or compression molded to form a part. LFT composites are now used in numerous high volume commercial applications in transportation, military, sporting goods and aerospace due to their lightweight characteristics, high specific modulus and strength, ease of processability, and recyclability [1-3].

In spite of their general use at ambient temperature, LFTs have also found their use in applications at elevated temperature. Glass fiber LFT (GF/nylon 66) has been used as a tailcone for an XM-1002 training round [4,5]. The LFT composite tailcone made of 40 wt% glass fiber reinforced nylon 66 was manufactured to replace aluminum counterpart using compression molding process. Skin temperature of the tailcone can reach up to 270°C for over 5 seconds during its flight. The flexural creep behaviors of GF/nylon 66 LFT, glass fiber reinforced polypropylene LFT, and glass fiber reinforced high density polyethylene LFT at elevated temperatures have been studied [6]. It is found that the long fiber composites exhibit non-linear viscoelastic response at moderate to high applied stresses and the addition of the long reinforcement fibers enhance the creep resistance [6]. Glass fiber reinforced PP LFT has also been used in the automotive industries as

underbody panel and dashboard [3,7] where temperature can rise up to over 60°C in hot summer days. Thin-walled shell made of CF/PAA LFT has to stand elevated temperature more than 100°C for durations up to 90 seconds [8].

In this study, long carbon fiber reinforced polyarylamide (CF/PAA) is used for the testing at elevated temperatures and consequent failure analysis is conducted. PAA, also known as PA-MXD6 which is a kind of nylon and produced from m-xylylenediamine and adipic acid through polycondensation reaction, is a semi-crystalline aromatic polyamide [9,10]. Currently there is no publication available that is related to the mechanical behavior of CF/PAA at elevated temperature. This research effort will be focused on systematically studying the effect of elevated temperature on the mechanical properties (flexural and tensile properties) of CF/PAA LFT samples in different orientations with different fiber contents and their failure mechanisms are evaluated.

### Material and Processing

20% and 30 wt% long carbon fiber PAA pellets supplied by Celanese were used to produce the plates from which the mechanical testing samples were prepared. All of the pellets have a length of 25 mm. In order to determine the proper processing and testing temperature of samples, it is necessary to understand the thermal properties and

**\*Corresponding author:** Ning H, Department of Materials Science and Engineering, University of Alabama at Birmingham, Birmingham, USA, Tel: 2059967390; E-mail: [ning@uab.edu](mailto:ning@uab.edu)

**Received** October 24, 2016; **Accepted** November 04, 2016; **Published** November 14, 2016

**Citation:** Wang Q, Ning H, Vaidya U, Pillay S (2016) Mechanical Behavior of Long Carbon Fiber Reinforced Polyarylamide at Elevated Temperature. J Material Sci Eng 5: 294. doi: [10.4172/2169-0022.1000294](https://doi.org/10.4172/2169-0022.1000294)

**Copyright:** © 2016 Wang Q, et al. This is an open-access article distributed under the terms of the Creative Commons Attribution License, which permits unrestricted use, distribution, and reproduction in any medium, provided the original author and source are credited.

stability of the CF/PAA using differential scanning calorimetry (DSC) and thermogravimetric analysis (TGA) before processing.

CF/PAA samples were analyzed using Q100 DSC (TA Instruments) for the melting temperature and glass transition temperature of PAA matrix. The CF/PAA sample was scanned from room temperature to 450°C at a rate of 10°C per minute. The resultant curve is illustrated in Figure 1. The melting of the PAA in the sample starts from approximately 270°C. The valley beginning at that temperature represents the melting endotherm for the CF/PAA sample. The sudden change of the heat capacity at the segment of 70-80°C corresponds to the glass transition temperature  $T_g$ . The peak at approximately 120°C is exothermic and represents crystallization of the PAA.

TGA (TA Instrument DSC Q100) was used to measure the degradation temperature of the PAA matrix. The sample was run in air environment and the temperature was ramped up at a rate of 10°C per minute. TGA was run to mainly evaluate the mass loss as a function of temperature. Figure 2 illustrates the mass loss as a function of temperature for CF/PAA and the mass loss dramatically increases at approximately 440°C.

Extrusion-compression molding process was used to manufacture the testing samples. Before processing, the pellets were dried for 24 hours at 90°C in a desiccant dryer to eliminate any moisture which could affect material processing and properties. Processing starts with

feeding the pellets into the hopper of a plasticator which has single screw and low shear. The pellets were metered down a barrel that was heated above the melting point and extruded in low shear. A temperature which is 30-40°C higher than the melting temperature of the PAA matrix was used for melting the PAA matrix to ensure adequate melting in the plasticator and flowing in the mold while avoiding any polymer degradation. The molten material was accumulated at the front end of the barrel and a specific amount of material was extruded and cut to a cylindrical-shaped charge. The extruded charge was transferred in a closed-cavity compression mold with the dimension of 305 mm by 305 mm housed within a heated hydraulic press under 60 tons pressure. The CF/PAA plate was then demolded after 5-minute dwell in the mold.

Multiple plates were used to prepare large number of samples needed for the flexural and tensile testing. In order to make sure that all the fibers have consistent orientation from plate to plate, the charge was placed at the same position and in the same orientation in the mold for every run. The direction along the axis of the cylindrical charge is defined as transverse orientation (90°), and the direction perpendicular to the axis of the charge (parallel to the charge flow direction) is defined as longitudinal orientation (0°). Figure 3 shows the schematic of the positioning of the charge and flow directions in relation to the orientation of the samples to be prepared for the mechanical testing.

Flexural samples were prepared according to ASTM D790-Standard Test Methods for Flexural Properties of Unreinforced and Reinforced Plastics and Electrical Insulating Materials. Tensile testing samples were prepared by cutting rectangular sample into dog-boned shape based on ASTM-D638 Standard Test Method for Tensile Properties of Plastics. Figure 4 shows representative flexural and tensile testing samples.

## Results and Discussion

Three different temperatures were selected for the mechanical testing: room temperature (RT), glass transition temperature (TG), and medium temperature 65°C (MD) between room temperature and  $T_g$ . In addition, different fiber content (20 and 30 wt%) of the LFT and orientation (longitudinal and transverse) of the molded samples were also taken into account in this study. Three samples were tested for each material category.

A servo-hydraulic universal testing frame with a heating chamber was used for flexural testing at different temperatures. All of the CF/PAA samples were 180 mm in length, 15 mm in width and 4.5 mm in thickness. Support span length was 120 mm and the loading rate was 2 mm/min.

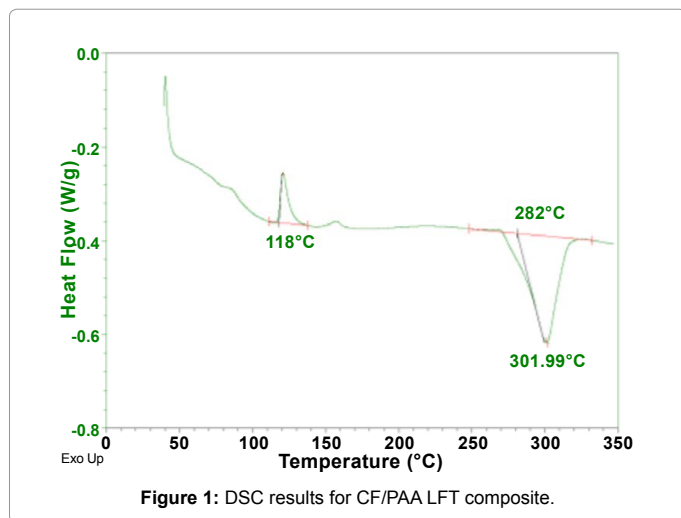


Figure 1: DSC results for CF/PAA LFT composite.

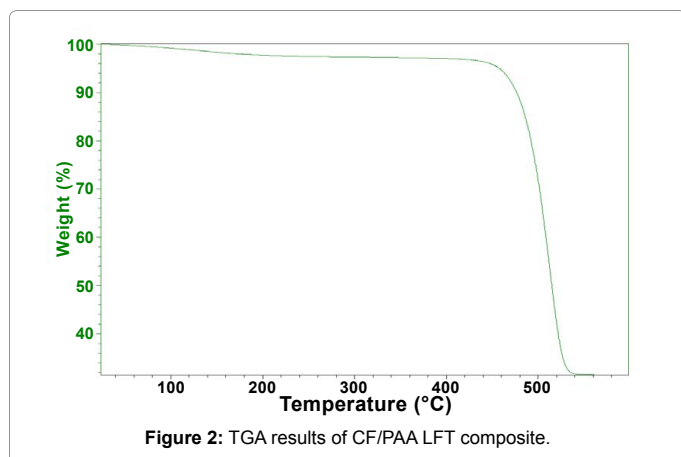


Figure 2: TGA results of CF/PAA LFT composite.

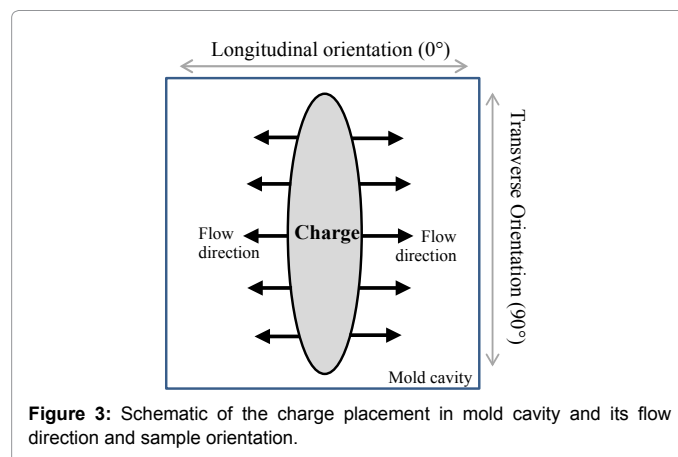


Figure 3: Schematic of the charge placement in mold cavity and its flow direction and sample orientation.

Tensile testing was conducted using the same testing frame and an extensometer was attached to the sample for obtaining the strain data during tensile testing, which was used to calculate tensile modulus. The sample was loaded at a loading rate of 2 mm/min.

Typical flexural load-displacement curves of 20 wt% CF/PAA samples in longitudinal ( $0^\circ$ ) orientation are presented in Figure 5. It is seen that the RT samples show linear load-displacement curve until catastrophic fracture when peak load is reached, indicating the rigid and brittle characteristic of the CF/PAA LFT composite at ambient temperature. However, the samples tested at the other two temperatures show nonlinearity, especially the ones tested at  $T_g$ , which indicates that their matrix softens and the interface between fiber and matrix weakens. The curves at glass transition temperature ( $T_g$ ) exhibit obvious ductile material characteristic fracture with higher strain to failure. Zig-zag patterns on the  $T_g$  curves indicates that there is continuous debonding between fiber and matrix due to weakened fiber-matrix interface at elevated temperature. The slope of the load-displacement curve at the RT temperature possesses the highest value while the lowest at  $T_g$  temperature. There is a change in the shape of the curves as a result of increasing testing temperature. The slopes of the curves decrease with increasing temperatures, indicating lower stiffness at higher temperatures. Peak load is reduced with increasing temperatures. Below  $T_g$ , PAA is in a glassy state which results in the highest stiffness and strength of the CF/PAA LFT composite.

Effect of temperature on the flexural strength of both 20 and 30 wt% samples is presented in Figure 6. The average flexural strength values

are plotted and compared along with the standard deviation added as the error bar. Temperature significantly affects flexural strength at the elevated temperature section between MD and  $T_g$  temperature. The samples in  $0^\circ$  orientation show that flexural strength drops 10% at  $65^\circ\text{C}$  for 20% CF/PAA and 5% for 30% CF/PAA, respectively. However, when temperature reaches  $T_g$ , flexural strength drops 26% and 64% for 20% CF/PAA and 30% CF/PAA, respectively. For the samples in  $90^\circ$  orientation, the reductions are 11% and 8% for 20% CF/PAA and 30% CF/PAA at  $65^\circ\text{C}$ , respectively, and dramatically increase to 43% and 68% at  $80^\circ\text{C}$ . The change in the shape of the curves as a result of increasing the temperature does not follow a linear trend. The property decreases exponentially when the temperature increases from 65 to  $80^\circ\text{C}$ .

Effect of temperature on the flexural modulus of the samples is presented in Figure 7. It is seen that flexural modulus is also largely affected by temperature and its reduction is much more as compared with that of flexural strength. In  $0^\circ$  orientation, flexural modulus drops 21% and 17% at  $65^\circ\text{C}$  for 20% CF/PAA and 30% CF/PAA, respectively. However, when temperature reaches  $T_g$ , flexural modulus drops 42% and 75%, respectively. In  $90^\circ$  orientation, the reductions are 40% and 40% for 20% CF/PAA and 30% CF/PAA at  $65^\circ\text{C}$ , respectively, and dramatically increase to 71% and 68% at  $80^\circ\text{C}$ . This again shows the non-linearity for the effect of temperature on flexural modulus.

A similar behavior to that of flexural load-deflection curves is

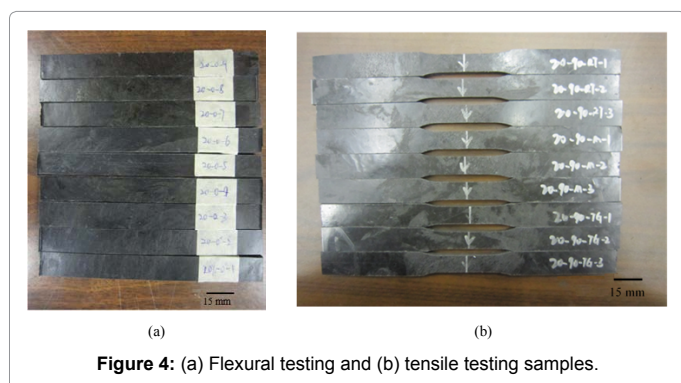


Figure 4: (a) Flexural testing and (b) tensile testing samples.

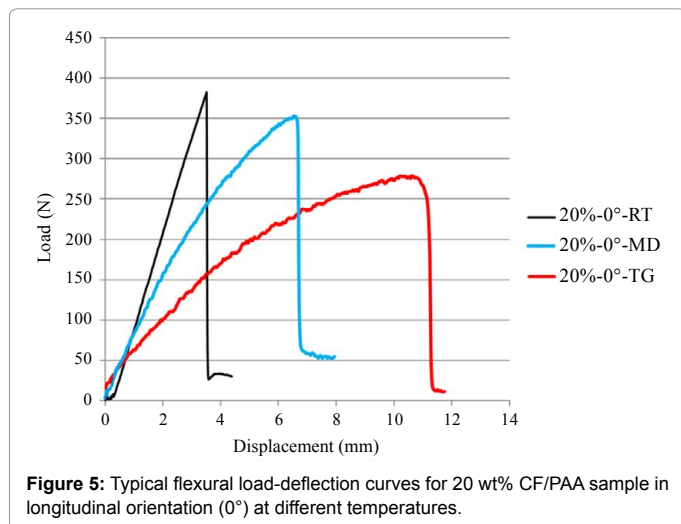


Figure 5: Typical flexural load-deflection curves for 20 wt% CF/PAA sample in longitudinal orientation ( $0^\circ$ ) at different temperatures.

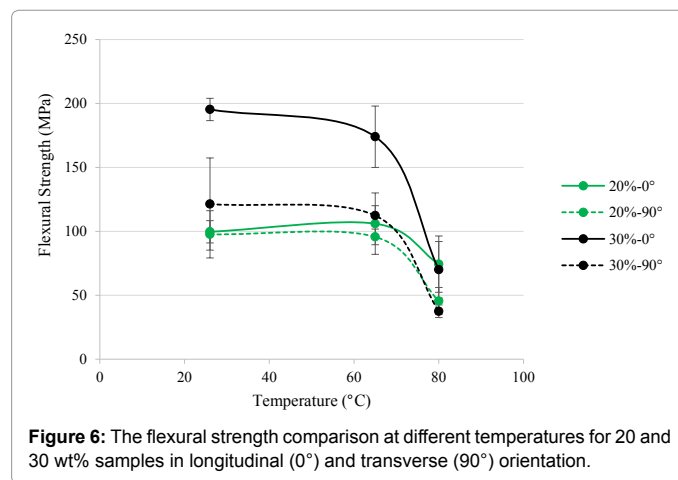


Figure 6: The flexural strength comparison at different temperatures for 20 and 30 wt% samples in longitudinal ( $0^\circ$ ) and transverse ( $90^\circ$ ) orientation.

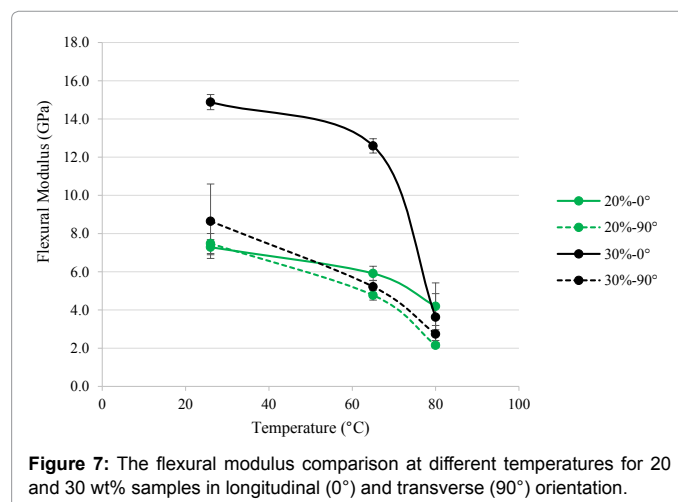


Figure 7: The flexural modulus comparison at different temperatures for 20 and 30 wt% samples in longitudinal ( $0^\circ$ ) and transverse ( $90^\circ$ ) orientation.

noticed for tensile testing results. As expected, the modulus of elasticity of the samples was reduced with increasing temperature. Figure 8 exhibits the effect of temperature on the tensile strength of the samples in both orientations. Tensile strength drops around 7 and 12% at MD temperature for samples containing 20 and 30 wt% carbon fibers in 0° orientation, respectively, and drops 10 and 15% in 90° orientations, which are very close to the reduction values of flexural strength. When the temperature is reached to T<sub>g</sub>, the corresponding reductions are 30% and 40% for 20% CF/PAA and 30% CF/PAA at 65°C, respectively, and still remain similar at 40% and 50% at 80°C, indicating that tensile strength is less affected by temperature compared to its flexural counterpart. It is understood that tensile modulus and strength are fiber-dominated property [11]. Tensile property is not as much affected as flexural properties which are matrix-dominated properties at elevated temperature, especially when the matrix PAA softens significantly at T<sub>g</sub>.

Effect of temperature on the tensile modulus of the samples is illustrated in Figure 9. Comparing with the tensile strength, tensile modulus is more affected by temperature. Tensile modulus reduces by approximately 20 wt% and 30 wt% samples at MD temperature (around 24% and 26%, respectively). At T<sub>g</sub>, the corresponding reductions are 43% and 51%, respectively.

Figures 6-9 illustrate that both strength and modulus show higher value in longitudinal orientation compared to transverse orientation, although that trend is more obvious for 30 wt% fiber loading samples.

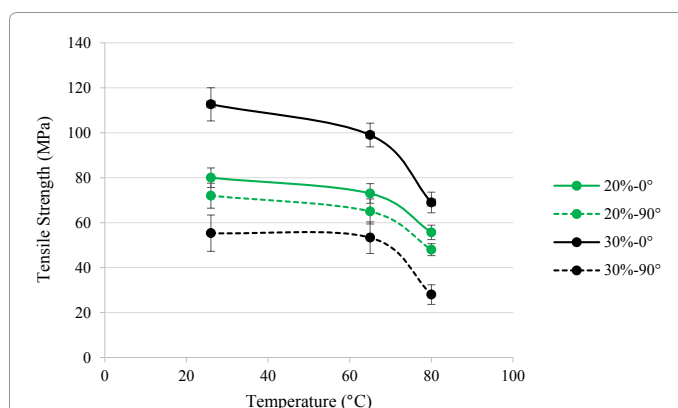


Figure 8: The tensile strength comparison at different temperatures for 20 and 30 wt% samples in longitudinal (0°) and transverse (90°) orientation.

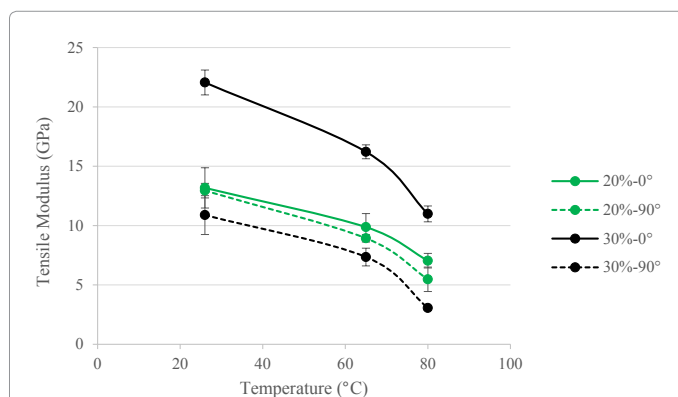


Figure 9: The effect of the temperature on the tensile modulus for 20 and 30 wt% samples in longitudinal (0°) and transverse (90°) orientation.

More fibers were oriented in the longitudinal direction because of the charge flow during compression molding which induces preferred fiber alignment in the flow direction. Thus, the properties of the samples in longitudinal orientation show higher mechanical properties. The samples in the transverse orientation have fewer fibers oriented in the loading direction and therefore lower property is resulted.

Generally it is found that the effect of temperature was more pronounced on the stiffness of composites (both flexural and tensile) as compared with that of strength values because of the fact that stiffness of the composite is directly related to the stiffness of the constituents which heavily depends on temperature. Strength is mainly governed by interfacial adhesion which is less influenced by temperature. Both of the strength and modulus have the highest decrease when the temperature is raised from MD temperature to T<sub>g</sub> temperature. Below T<sub>g</sub>, the interfacial bonding between the fiber and matrix is not much affected and PAA matrix is glassy below glass transition temperature. When temperature is reached to T<sub>g</sub>, the weakened interfacial bonding and softened matrix account for the large reduction in material properties. Similar trend of unidirectional fiber composite has been reported by other research groups. It was found that the longitudinal strength and modulus of a unidirectional laminate remain virtually unaltered with increasing temperature, but its transverse and off-axis properties are significantly reduced as the temperature approaches the T<sub>g</sub> of the polymer matrix [12].

Stereoscope was used to analyze the failure mechanisms of the samples tested at different temperatures. Figure 10 shows typical fracture surface of the flexural sample tested at RT and T<sub>g</sub> temperature (30% CF/PAA longitudinal samples). The fractured sample at RT temperature shows a typical brittle failure and there is no obvious fiber pull-out. However, the sample tested at T<sub>g</sub> has distinct fiber pull-out and delamination.

Scanning electron microscope (SEM) was also used to study the fracture surfaces of flexural test specimens. Figure 11 shows the SEM images of the same fracture surfaces shown in Figure 10. Both fracture surface of the specimens (30% CF/PAA samples in longitudinal orientation) were studied using a Quanta 650 FEG field emission scanning electron microscope. Figure 11a shows the fracture surface image of the sample tested at RT. It is noticed that the main failure mechanism is fiber fracture and there is also some fiber pull-out with polymer adhering to the fibers, indicating a good fiber-matrix bonding. However, the fracture surface of the flexural specimen tested at T<sub>g</sub> temperature (Figure 11b) show that fiber pull-out phenomenon

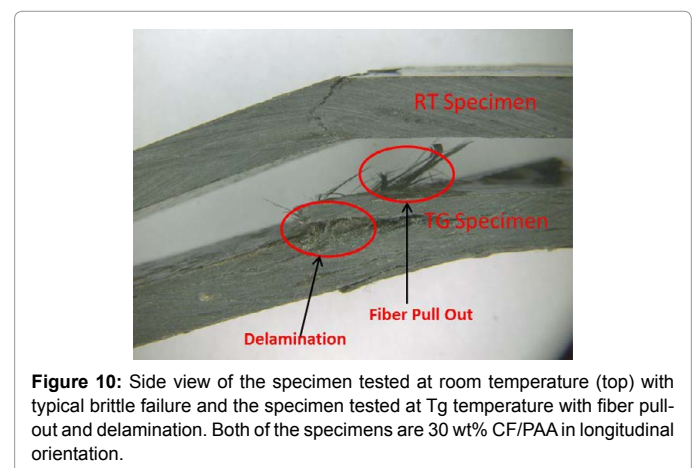
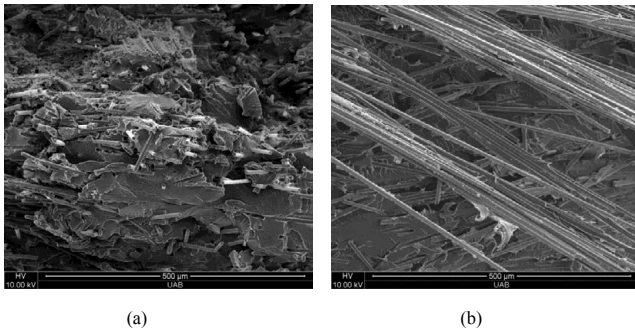
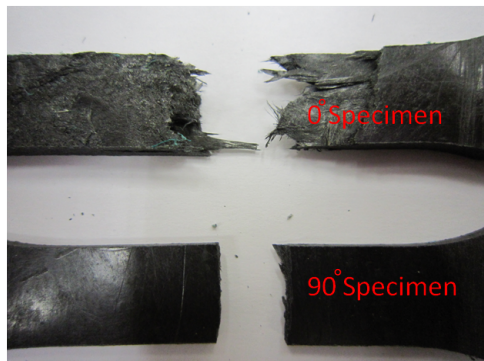


Figure 10: Side view of the specimen tested at room temperature (top) with typical brittle failure and the specimen tested at T<sub>g</sub> temperature with fiber pull-out and delamination. Both of the specimens are 30 wt% CF/PAA in longitudinal orientation.



**Figure 11:** (a) Typical SEM of fracture surface of flexure specimen tested at RT and (b) Typical SEM of fracture surface of flexure specimen tested at TG. Both of the specimens are 30 wt% CF/PAA in longitudinal orientation.



**Figure 12:** Typical fracture surface of tested tensile specimen in 0° (top) and in 90° (bottom) orientation. Both of the specimen have fiber loading of 30 wt% and are tested at MD temperature.

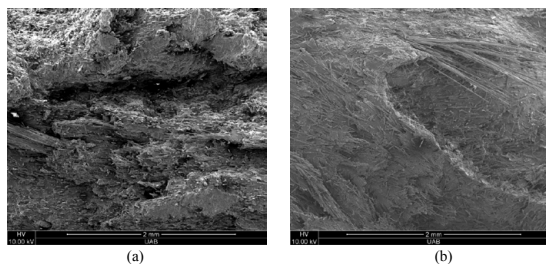


**Figure 13:** (a) SEM image of fracture surface of tensile specimen in 0° orientation; and (b) SEM image of fracture surface of tensile specimen in 90° orientation. Both of the specimens have 30 wt% fiber loading and are tested at MD temperature.

is dominant and there is minimum fiber fracture. The length of the fiber pulled out of the matrix is much longer than the fibers pulled out as shown in Figure 11a. It indicates that the bonding strength between fiber and matrix at elevated temperature was much weaker as compared to that at RT temperature and the pull-out is the main failure mechanism at elevated temperature.

Typical stereoscopic pictures of the tested tensile samples are shown in Figure 12 (30% CF/PAA). It is seen that these two samples have totally different morphology at the fracture surface. For the sample in 0° orientation, the fracture surface is not straight and there are obvious fibers exposed at the surface. However, the sample in 90° orientation has nearly straight fracture surface and no noticeable fibers

exposed. This indicates that there are a large number of fibers involved in the tensile test for the 0° orientation sample. The involvement of large number of fibers in the 0° samples results in higher mechanical properties than the 90° samples. Figure 13 shows the SEM images of the same tensile samples. Figure 13a shows the fracture surface of the sample in 0° orientation and it is noticed that a large number of fibers are exposed on the fracture surface as compared to the fracture surface of the sample in 90° orientation as shown in Figure 13b. This indicates that the main failure mechanism is fiber breakage for the sample in 0° orientation due to the fact that more fibers are oriented in 0°. During tensile testing, the fibers oriented in 0° mainly bear the tensile loading and therefore these 0° oriented samples show higher tensile strength and modulus. The fracture surface of 90° orientated samples is much smoother compared to 0° orientation sample. There is fewer fiber breakage compare to the 0° oriented sample and the main failure mechanism for the sample in 90° orientation is matrix fracture. In this case, fibers do not play a load-bearing role since few fibers are aligned in loading directions. As a result, the samples in 90° orientation show less strength and modulus.

## Conclusions

The effect of temperature on the mechanical properties of the carbon fiber reinforced polyarylamide was studied in this research. The CF/PAA samples were processed using extrusion-compression molding and tested in flexural and tension. The effect of sample orientation and weight percentage of carbon fibers on the flexural and tension properties were evaluated. The following conclusions are drawn from the results and discussion presented above: 1) Flexural strength, flexural modulus, tensile strength, and tensile modulus of the CF/PAA LFT composites reduce exponentially from medium temperature 65°C to glass transition temperature, 80°C; 2) The effect of temperature on both of flexural and tensile modulus of the composite is more pronounced compared with flexural and tensile strength; 3) The reduction of both strength and modulus in 90° orientation samples is larger than in 0° orientation samples; 4) Flexural properties of the composites were influenced by temperature to a higher degree than tensile properties.

## Acknowledgements

The authors would like to thank Department of Energy (DOE) Graduate Automotive Technology Education (GATE) program for funding this research.

## References

- Hartness T, Husman G, Koenig J, Dyksterhouse J (2001) The characterization of low cost fiber reinforced thermoplastic composites produced by the DRIFT™ process. *Compos Part A: Appl S* 32: 1155-1160.
- Steffens M, Himmel N, Maier M (1998) Design and analysis of discontinuous long fiber reinforced thermoplastic structures for car seat applications. *Transactions on Engineering Sciences* 21: 35-44.
- Thattai parthasarathy KB, Pillay S, Ning H, Vaidya U (2008) Process simulation, design and manufacturing of a long fiber thermoplastic composite for mass transit application. *Compos Part A: Appl S* 39: 1512-1521.
- Sands JM, Vaidya U, Husman G, Serrano J, Brannon R (2008) Manufacturing of a composite tailcone for an XM-1002 training round.
- Vaidya UK, Serrano JC, Villalobos A, Sands J, Garner J (2008) Design and analysis of a long fiber thermoplastic composite tailcone for a tank gun training round. *Mater Des* 29: 305-318.
- Chevali VS, Dean DR, Janowski GM (2009) Flexural creep behavior of discontinuous thermoplastic composites: Non-linear viscoelastic modeling and time-temperature-stress superposition. *Compos Part A: Appl S* 40: 870-877.
- Henning F, Ernst H, Brüssel R (2005) LFTs for automotive applications. *Reinf Plast* 49: 24-33.
- Ning H, Pillay S, Vaidya U, Andrews JB (2008) Processing and characterization of thin-walled long fiber reinforced thermoplastic (LFT) composites, in International SAMPE Symposium.

- 
9. Xi Z, Chen L, Zhao Y, Zhao L (2013) Experimental and modeling study of melt polycondensation process of PA-MXD6, in Macromolecular Symposia. Molecular Symposia 333: 172-179.
  10. Doudou B, Dargent E, Grenet J (2006) Crystallization and melting behaviour of poly (m-xylene adipamide). J Therm Anal Calorim 85: 409-415.
  11. Kumar BG, Singh RP, Nakamura T (2002) Degradation of carbon fiber-reinforced epoxy composites by ultraviolet radiation and condensation. J Compos Mater 36: 2713-2733.
  12. Mallick PK (2007) Fiber-reinforced composites: materials, manufacturing, and design. CRC press, USA.